

Chapter 14

A Method for Overlapping Two DIC Views by Using a Two-Tone Speckle Pattern

Phillip L. Reu

Abstract Because both the accuracy and spatial resolution of digital image correlation (DIC) are directly related to the field-of-view and the number of pixels, it is sometimes advantageous to have a tight view for high resolution measurements and a wide view for overall object deformation. This approach will be demonstrated using a high-speed measurement of the deformation and strain of a riveted thin plate with an explosive loading. Overall plate deformation was provided by a wide-view stereo system, while a tight view of a section of the rivets was imaged with a second stereo pair to measure the strain around the rivet holes. The challenge is creating a speckle pattern which will work with both systems without creating holes in the overall measurement data. This was accomplished by creating a black/white coarse pattern for the wide view and a black/grey/white fine pattern for the tight view. The grey speckles were sized such that they are not resolved by the wide view and therefore do not compromise the full-field measurement. Details of the process and example results will be presented.

Keywords Digital image correlation • Uncertainty quantification • Photogrammetry • DIC • High-speed

14.1 Introduction

Digital Image Correlation (DIC) is a full-field photometric measurement technique. Fundamentally the resolution of the technique is related to the pixel size on the object. Therefore, to increase the displacement resolution it is important to maximize the number of pixels across the sample (all other things being equal). The use of DIC with widely available high-speed cameras has led to its increased use in explosive research. This technique has been used at Sandia National Laboratories to gain a more complete understanding of blast loading. To best quantify the loading on a plate, it is important to know both the overall deformation of the object, as well as be able to measure strain around small features. Due to limitations in the number of pixels available in high-speed imaging, this requires two radically different fields-of-view (FOV). This paper discusses a two-tone paint scheme with different speckle sizes to allow two overlapping views from two DIC stereo-systems. This maintains the primary measurement of the deformation of the entire paint surface, while allowing strain to be measured around rivets in the middle of the plate.

14.2 Experimental Setup

14.2.1 Explosive Test Stand and Stereo-rigs

Sandia National Laboratories has developed an explosive test stand for measuring the reaction of 1.2 m diameter plates to an explosive blast. The stand consists of a massive steel frame on which the plate can be bolted. The stand includes a large area around the plate for measurement of the stand movement, as well as delaying the arrival of the blast products into the

P.L. Reu (✉)
Sandia National Laboratories, PO Box 580087185 Albuquerque, NM 87185, USA
e-mail: plreu@sandia.gov

Fig. 14.1 Stereo-rig setup behind protective wall



measurement area. Two DIC stereo-rigs were positioned approximately 6 m from the sample behind a protective wall with thru-holes for the cameras to observe the deformation of the plate surface during the blast loading. The camera position behind the wall provided adequate protection for the cameras, without the use of Lexan viewports. An analysis in Sect. 14.2.3 demonstrates why Lexan should be avoided if possible in DIC applications. The stereo-rig consisted of a beam on which all four cameras were rigidly mounted as shown in Fig. 14.1. The wide stereo-rig was composed of two Phantom v12 cameras with 35–80 mm zoom lenses and was run at a resolution of 368×360 pixels and 37,012 frames-per-second (fps). The tight stereo-rig used two v1610 cameras with 400 mm lenses, with a resolution of $1,280 \times 720$ pixels, and a frame rate of 18,500 fps. The sample area was shaded by a large tent structure to prevent shadows on the surface that greatly compromise the DIC results. Ambient light in the shade was still adequate to have an exposure of 15 μ s for the wide view and 47 μ s for the tight view.

14.2.2 DIC Speckling for Two Fields-of-View

The experimental design required that the displacement of the plate be maintained over the entire FOV to match the data acquired in previous tests, however, rivets on the plate, required a smaller FOV in order to capture their deformation and strain. The difficulty in doing this is that speckles optimized for one FOV are almost never adequate for a different size. This is because the goal is to have 3–5 pixels per speckle in order to optimize the spatial resolution of DIC by using the smallest effective subset size and step size, which leads to the smallest possible virtual gage size. The wide FOV had a pixel size on the object of 4 mm/pixel, which gives an optimal speckle size of between 12 and 20 mm. The tight FOV has a 0.4 mm/pixel size at the object, with an optimal speckle size of 1.2–2 mm. In this, case, because the pixel sizes at the object were so radically different, the small speckles for the tight view were small enough, $\frac{1}{2}$ -pixel or less in the wide view that they were not seen by the cameras – and appeared as a hazy area in the image (see left side and inset of Fig. 14.2). To create an appropriate speckle at the small FOV, a grey paint was used in order to have speckle contrast over both the large black speckles and the white areas between the speckles from the wide view speckle pattern. Of course, with this approach, there is a compromise in the contrast that may negatively impact the results. However, with 12-bit cameras and good lighting, there was plenty of dynamic range using the grey speckles, yielding 700 grey levels between the white and grey and another 700 grey levels between the grey and black. The match quality for this contrast was estimated by the DIC software to be 0.01 pixels.

14.2.3 The Effect of Lexan on DIC Results

There is no question that protecting expensive high-speed cameras during explosive testing is important, however, placing cameras behind Lexan *will* affect the results. This is due to the optical distortions caused by the Lexan and results from either the inherent optical defects of the material, or by bending the Lexan during mounting. It is important to quantify the influence of the Lexan on the results. For this experiment, the error was quantified by calibrating both with and without the Lexan in place, and acquiring images of a flat speckle target, translated in the FOV. The calibration using the same board yielded two different projection error scores; with Lexan it was 0.088 pixels and without Lexan it was 0.037 pixels. This is

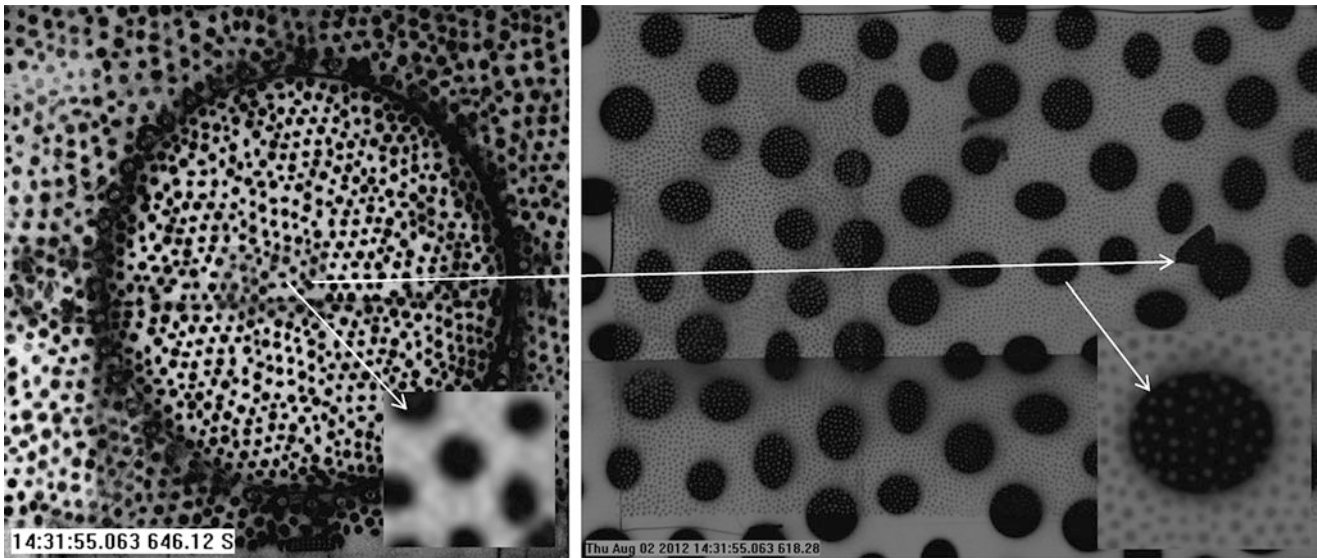


Fig. 14.2 Speckle patterns for both the (*left*) wide view showing unresolved small speckles as a hazy region and (*right*) tight view showing the resolved three-tone speckle pattern. Insets on both figures show a detailed region of the two-tone speckle region

Table 14.1 Error summary of Lexan

	Lexan	Lens Only
Average Projection	0.045	0.014
Max Projection	0.054	0.027
Average U Error 2σ	0.487	0.108
Average V Error 2σ	0.589	0.091
Average W Error 2σ	1.195	0.478
Max U Error	1.282	0.247
Max V Error	1.148	0.297
Max W Error	3.077	1.128

almost certainly caused by issues with fitting the non-radial lens distortions to the available radial distortion parameters during the bundle adjustment calibration. A flat board was then translated in the FOV and images were acquired both with and without the Lexan. The images were analyzed using DIC software, an average projection error of 0.05 pixels was obtained with the Lexan and 0.02 pixels without the Lexan. Again, indicating a compromise in the results due to the added optical distortions. A best-fit plane was used to transform the data from the camera coordinates to the flat plate, and then rigid-body motions were removed. For a flat plate that remains flat, this will primarily yield the errors due to the optical distortions. These errors are summarized in Table 14.1 and illustrated for the Z-direction in Fig. 14.3. The figure clearly shows that there is a 3 mm error in the out-of-plane direction caused only by the Lexan distortion. For reference – the pixel size at the object is 4 mm/pixel.

14.3 DIC Results

The plate with a lap rivet joint (6.35 mm rivets with 30 mm spacing) was loaded by an explosive charge behind the sample. The wide stereo-rig successfully captured the motion of the plate, with no loss of data in the high resolution region. The tight stereo-rig also yielded data throughout its FOV. The results from the two systems were compared using a line cut taken from the DIC data at a short period after the loading began. Figure 14.4 shows the out-of-plane results for two frames from the wide view and one from the tight view. The smoothing of the data over the lap joint is clearly seen in the wide view, because

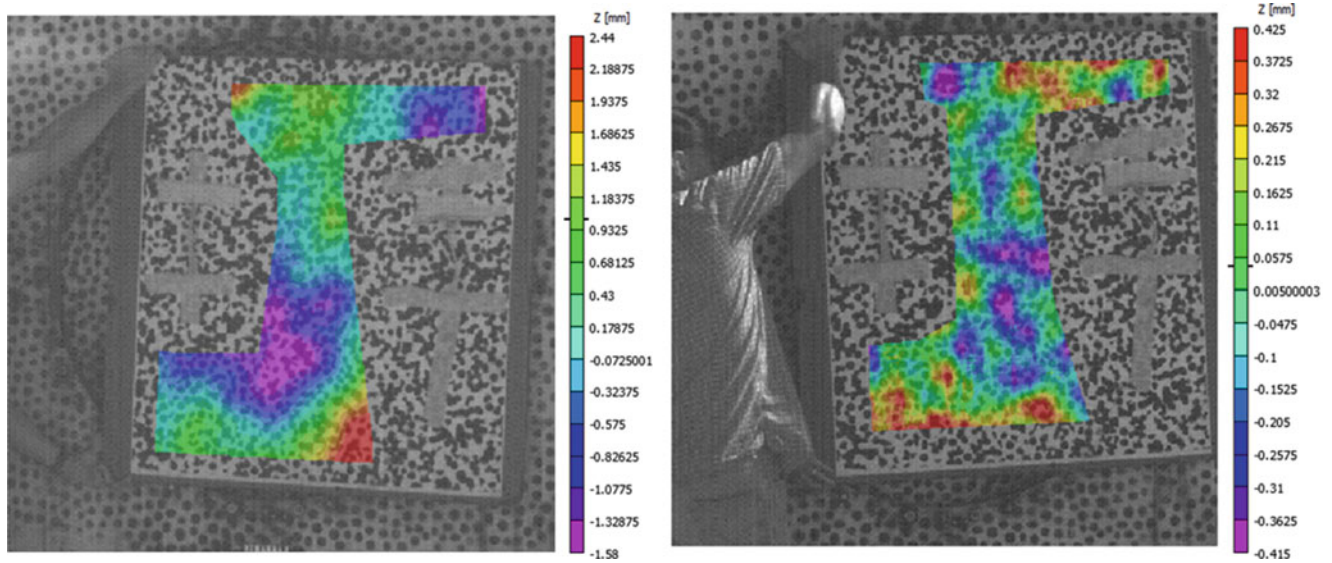


Fig. 14.3 (Left) False shape caused by Lexan distortions. (Right) DIC displacement noise

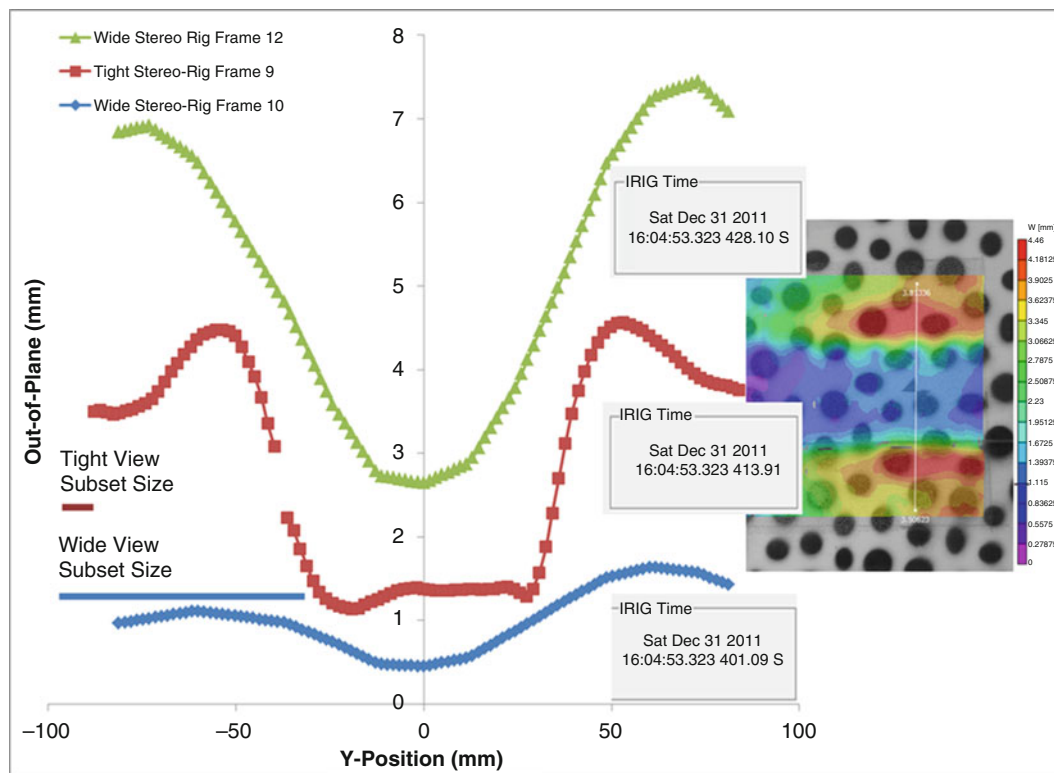


Fig. 14.4 Line cut comparing the out-of-plane displacement of the two FOVs along the illustrated line-cut. Also shown are the subset size on the same scale as the y-dimension

of the relatively large 68 mm subset size (illustrated in the figure), which bridges the high deformation gradient around the lap joint. The step size for the wide view was 3-pixels (12 mm), which yields only 16 data points across the dimension shown in Fig. 14.5. The added data points are interpolated. The tight view is better able to represent the displacements at the lap joint because the subsets are physically much smaller (11.6 mm) as illustrated in Fig. 14.5. This figure clearly illustrates the importance of spatial resolution on the accuracy of the DIC results.

Fig. 14.5 Illustration of virtual gage size on the stain gradients (ϵ_{yy}) same load step analyzed with different virtual gage sizes and plotted with the same scale

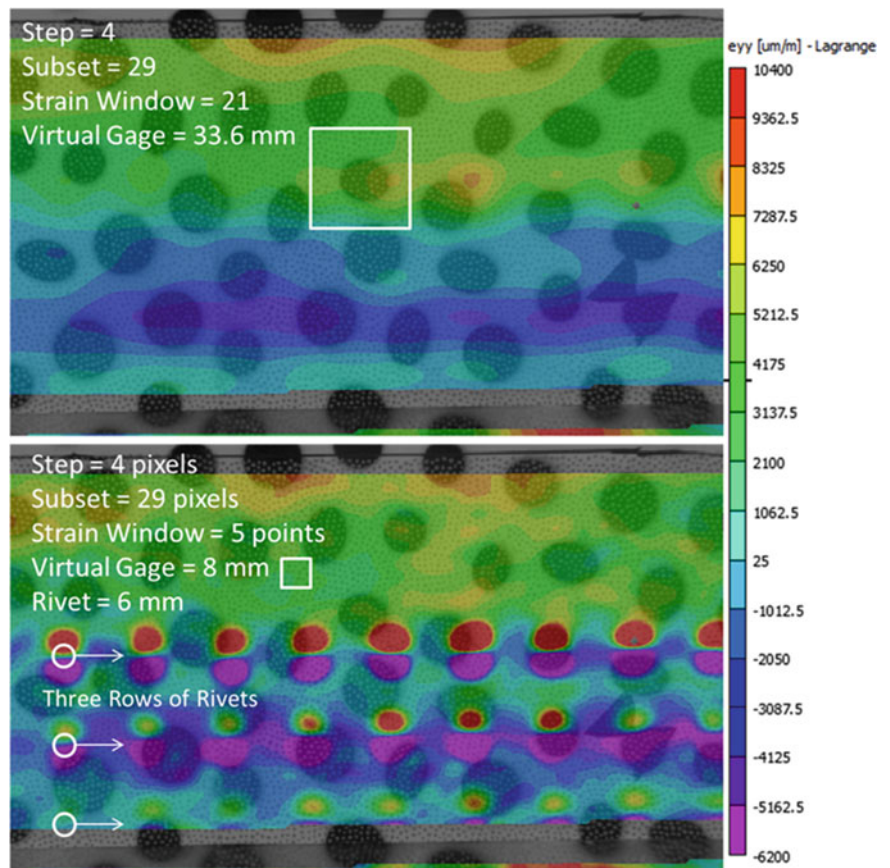
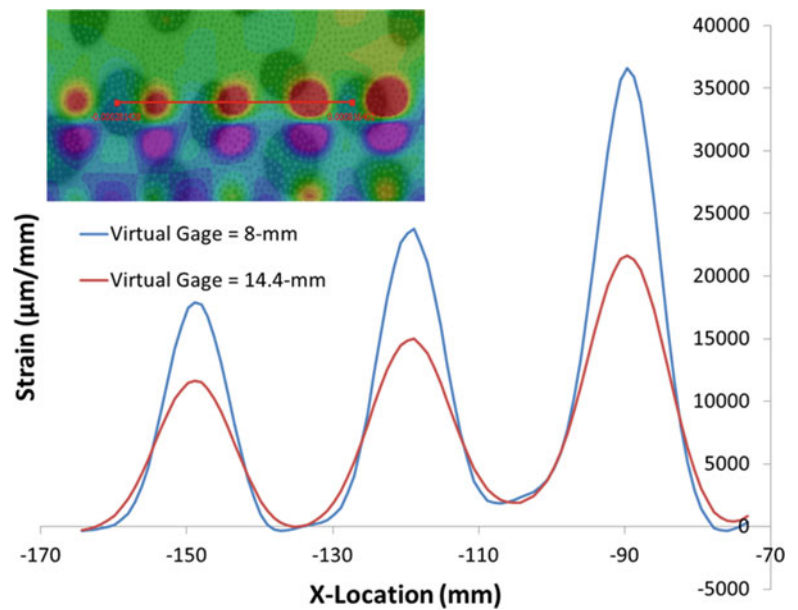


Fig. 14.6 Virtual gage size study. Red line is the extracted region plotted



Spatial resolution is even more critical for the strain results, where a region of the DIC displacement results (the virtual gage) is fit before taking a derivative to calculate the strain. The wide view with a strain window of 15 data points would yield a virtual gage size of 180 mm – valid only for giving average strain at best. For the tight FOV, virtual gages of 8 mm are possible and better able to capture the strain gradients around the rivets. Figure 14.6 clearly illustrates the effect of the virtual

gage size on the strain results for two different sizes. Obviously the smaller gage better captures the strain gradients between the rivets, however, to determine where the strain is correct, a “mesh density” type study was done by varying the virtual gage size and is shown in Fig. 14.7. The strain accuracy can be determined by looking for regions where the strain is identical regardless of gage size. Any matching strains are accurate; any non-matching strains are a minimum estimation of the strain.

14.4 Conclusions

A two-tone speckle pattern was used to create overlapping DIC fields-of-view. Due to the tenfold difference in pixel size at the object, the wide view was unable to image the small pattern used for the tight view, yielding data across the entire surface. The tight view was able to image a small enough area that strain was able to be measured around small rivets, which would be completely un-measurable with a single wide FOV. This was illustrated by doing a virtual strain gage size study and looking at the variation in the strain results. An analysis of the influence of Lexan viewports was also completed, showing for this case that the bias errors due to the Lexan would be unacceptably large.

Acknowledgements I would like to thank Michael Bejarano for setting up the DIC experiment and acquiring the images.

Sandia is a multiprogram laboratory operated by Sandia Corporation, a Lockheed Martin Company, for the United States Department of Energy under contract DE-AC04-94AL85000.